ORIGINAL PAPER

Dynamic response of beams under moving loads with finite deformation

Yuanbin Wang · Xiaowu Zhu · Zhimei Lou

Abstract A novel material parameter-dependent model is proposed in this work to investigate the nonlinear vibration of a beam under a moving load within a finite deformation framework. For the planar vibration problem, the Lagrange strain is adopted and the resulting model equations for the beam are established by the Hamilton principle. Under appropriate assumptions, the coupled model equations are simplified into a nonlinear integro-partial differential equation which incorporates a material parameter and a geometrical parameter. The dynamic response of the beam is determined with the help of the Galerkin method. The solutions show that both the material parameter and geometrical parameter have the effect of reducing the amplitude of the forced vibration, increasing the speed of the fluctuation and the critical velocity for the moving load. In comparison with small deformation formulations, the effect of finite deformation herein is to reduce the vibration amplitude, especially for slender beams. If the vibration amplitude is relatively small, the nonlinear

model may be replaced by the corresponding higher-order linear model while preserving the main features of the vibration problem.

1 Introduction

The dynamic response of beams under moving loads has been analyzed extensively during the past decades, owing to its applications in engineering systems such as bridges traveled by vehicles or pedestrians, space tethers, satellite antennas, launch systems and so on. In Fryba [1], various analytical solutions for vibration problems of simple and continuous beams under moving loads were documented. Recently, Ouyang [2] also reviewed the vibrations of beams under moving loads. It is beyond the scope of this article to present an exhaustive literature review, one can refer to [3–11] for more information. The most relevant work discussed below is classified according to the beam models they adopt, which mainly include the Euler beam theory, Timoshenko beam theory and some higher-order shear deformable beam theories.

Based on the Euler beam theory, an abundant body of work has been reported on the vibrations of beams subjected to moving loads, either in a linear or nonlinear setting. For example, Sheng and Wang [12] numerically examined the nonlinear dynamic responses of Kelvin–

Y. Wang
Department of Mathematics, ShaoXing University,
Shaoxing, Zhejiang, People's Republic of China

X. Zhu (✉)
School of Statistics and Mathematics, Zhongnan University
of Economics and Law, Wuhan 430073, Hubei,
People's Republic of China
e-mail: xiaowuzhu1026@znufe.edu.cn

Z. Lou
Department of Physics, ShaoXing University, Shaoxing 312000,
Zhejiang, People's Republic of China

Voigt beams under moving loads. They found that the dynamic responses of the nonlinear model were higher than those of the linear model. Eftekhari [13] applied the differential quadrature method to investigate the steady state of the linear and nonlinear vibration of Euler–Bernoulli Von Karman beam resting on an elastic Winkler foundation; the beam was subjected to a moving point load. Di Lorenzo et al. [14] studied the vibration response of the Euler uniform beam under moving loads with Kelvin–Voigt viscoelastic supports. The free vibration solutions and dynamic responses were obtained by numerical methods. The velocity of the moving load plays a very important role in determining the vibration of the beam, and substantial work is available that investigates the dynamic response of the beams at the critical state. Timoshenko [15] firstly studied the steady-state solutions of the dynamic response of a beam on an elastic foundation under a moving load. These results showed that at the critical velocity (of the moving load), the deflection of the beam becomes larger. Later, many researchers studied the steady state of the beam and the critical velocity of the moving load. Kenney [16] investigated the steady-state vibrations of a beam under a moving load. Crandall [17] obtained the steady-state solutions for a Timoshenko beam on an elastic foundation with a moving concentrated load. In [18], Achenbach and Sun studied the effect of the damping coefficient and the velocity of the moving load on the dynamic response of a Timoshenko beam on a flexible support. Steele [19] studied the steady-state solutions at the critical state and obtained the asymptotic solutions. Dieterman and Metrikine [20] obtained two critical velocities of a constant load moving at a constant speed along a Euler–Bernoulli beam. As to the critical velocity which leads to the largest vibration amplitude, some remarkable results were obtained in [21,22]. Based on the Euler beam model, Rodrigues et al. [21] and Froio et al. [22] studied the dynamic response of beams on elastic foundations under an oscillating and concentrated moving load, the effects of the foundation's stiffness and damping on the critical velocity were investigated. With the help of Fourier transform, Dimitrovovà [23], Dimitrovovà and Rodrigues [24] studied the critical velocity of a uniformly moving load on an infinite Euler beam which was supported by a finite depth foundation. Chen and Huang [25] applied the dynamic stiffness matrix method to study the dynamic characteristics of Timoshenko beam on a viscoelastic foundation and determined the critical velocity. Tekili et al. [26] studied the nonlinear vibration of aluminum beams strengthened by carbon coats under moving loads at a constant speed. In order to take into account the effect of the shear deformation on the vibration of beams, Timoshenko beam theory is widely used. Kim et al. [27] applied the modal analysis method to study the dynamic responses of a Timoshenko beam under a moving load. The natural frequencies and mode shapes were obtained in closed forms. Ding et al. [28] investigated the dynamic response of infinite Timoshenko beams under moving loads supported by nonlinear viscoelastic foundation, and the dynamic response of the beam was obtained.

As mentioned above, in most of the literature the deformation of beams under moving loads or mass is described either by the Euler or Timoshenko beam theory. However, it is well known that the shear deformation of the beam is neglected in Euler beam theory, while the Timoshenko beam theory is based on an average shear strain. Furthermore, the cross section of the beam is assumed to remain planar after deformation in both of these theories. In addition, both the Euler and Timoshenko beam theories do not accurately capture the vibration response of the beam when the force is large. To overcome such drawbacks, higher-order shear deformable beam theories have been adopted to study the dynamic response of beams under moving loads. For the finite Timshenko–Rayleigh beam, Sapountzakis and Kampitsis [29] studied the nonlinear response of beams under moving loads resting on a nonlinear three-parameter viscoelastic foundation. Tabejieu et al. [30] applied the standard averaging method to study the response of a Rayleigh beam, subjected to moving loads, that is resting on a fractional-order viscoelastic Pasternak foundation. Hryniewicz [31] studied the dynamic response of Rayleigh beams resting on nonlinear viscoelastic foundations under moving loads. Based on a refined beam model and taking into account the effect of the thermal and elastic foundation, Chen et al. [32] investigated the nonlinear dynamic response of functionally graded tubes under moving loads by the Galerkin method.

Although existing higher-order shear deformable beam theories take into account the shear deformation and rotation inertia of the beam, the effect of the material parameter on the deformation is not considered. Moreover, as far as the authors are aware of, most of the literature investigating the moving load-

induced vibration problem considers the geometrical nonlinear effect, but little is available on exploring the dynamic response in a finite deformation setting. One of the important engineering problems which can be modeled as a simply supported beam undergoing large deformations under a moving load is the vehicle-bridge structure. For this structure, the moving vehicle (e.g., a train) is ideally treated as a moving load which is imposed on the (beams of the) bridges or roads. Nowadays, some lighter and slender beams are widely used in roads and bridges. The slender beams may be subject to a large deformation when the load or mass moves along it. Furthermore, the dynamic response could become more severe than that of the static loading case. In view of this, it is most desirable to analyze the vibration of the beam in the framework of finite deformation. However, most of the existing models in the literature only consider the nonlinearity that arises from the nonlinear foundations, without considering nonlinear deformations of the beam. Thus, for forced nonlinear vibration of beams, higher-order model equations established in finite deformation settings are crucial in analyzing the nonlinear dynamic response. At this time, a model to support this analysis is not available in the literature, which motivates the present work.

In this paper, a recently developed beam theory [33] (see also [34] for axially moving hyperelastic beams), which takes into account the shear deformation and the characteristics of the material, is applied to explore the nonlinear vibration of beams that are subjected to moving loads with finite deformation. The investigation reveals that both the material parameter and finite deformation are important in exploring the dynamic response of the beam. The arrangement of the remaining parts of this article is as follows. In Sect. 2, in the framework of finite deformation, the model equation for planar vibration of a beam under a moving load is derived through the Hamilton principle. With simply supported boundary conditions, the model equation is decoupled and simplified into a single integro-partial differential equation of the transverse displacement at the neutral axis. Several simplified models are also presented in this section. In Sect. 3, with the help of the Galerkin method, the model equation is transformed into a set of ordinary differential equations. The effects of the material parameter, the geometrical parameter and finite deformation on the forced and free vibrations

are discussed. Finally, some conclusions are drawn in Sect. 4.

2 Model equations

A beam with simply supported boundaries under a moving load P (with a constant transport velocity γ) is considered in the present study. The beam is assumed to have length L, density ρ and uniform cross section A. The x-coordinate is taken along the length of the beam, and the y-coordinate is taken along the thickness of the beam. The longitudinal and transverse displacements of the beam at time t are denoted by $u_1(x, y, t)$ and $u_2(x, y, t)$, respectively. For simplicity, only the in-plane dynamic behavior of the beam is considered in the model, while the out-of-plane motion and vibration are not taken into account.

2.1 Model equations based on finite deformation

As reviewed in Sect. 1, the Euler–Bernoulli beam theory, Timoshenko beam theory, Reddy beam theory and some other higher-order shear deformable beam theories are usually adopted to study the dynamic behaviors of beams under moving loads. However, one drawback of these beam theories is that the effect of the material parameter on the deformation is not taken into account. In fact, the displacement in the axial direction may affect the lateral displacement through material parameters, e.g., Poisson's ratio. In order to overcome this limitation, a material parameter-dependent kinematic frame proposed in [33] is applied to describe the deformation of the beam as follows

$$\begin{cases} u_1(x, y, t) = u_0(x, t) - yw_{0x}(x, t), \\ u_2(x, y, t) = w_0(x, t) - y\nu(u_{0x}(x, t) \\ \quad - \frac{1}{2}yw_{0xx}(x, t)), \end{cases} \quad (1)$$

where u_0 and w_0 are, respectively, the longitudinal and transverse displacements of the beam at the neutral axis $y = 0$. The parameter ν is the in-plane Poisson's ratio of the material. For isotropic materials, ν is defined as the ratio of the lateral strain in the y direction to the axial strain in the x direction. Hereafter, the subscripts x, y and t are used to denote the derivatives with respect to x, y and t, respectively.

Obviously, kinematic frame (1) reduces to the Euler beam theory when $\nu = 0$. It is to be noted that, in kinematic frame (1), the effect of the longitudinal displacement u_0 on the transverse displacement w_0 is taken into account. Also, as the cross section of the beam does not remain planar after deformation and does not remain normal to the deformed neutral axis, this implies that the shear deformation of the beam is considered in this frame. The detailed explanation of this issue as well as comparisons with shear deformable beam theories is included in "Appendix A". Furthermore, only two unknowns u_0 and w_0 are involved in the frame, which is less than alternative higher-order shear deformable beam theories (e.g., the Timoshenko beam theory has three unknowns). Thus, it is expected that the complexity of the resulting governing equations for the model may be reduced. The results in [33,34] also show that (1) can produce more accurate results for the displacements than some other theories, as it takes into account the effects of material parameter ν, the shear strain and the rotation strain.

In order to describe the nonlinear vibration problem, the Lagrange strain $\mathbf{E}$ is used in this paper, and it is given by

$$\mathbf{E} = \frac{1}{2}(\mathbf{F}^T\mathbf{F} - \mathbf{I}), \tag{2}$$

where the deformation gradient tensor can be calculated as

$$\mathbf{F} = \begin{pmatrix} 1 + u_{1x}(x, y, t) & u_{1y}(x, y, t) & 0 \\ u_{2x}(x, y, t) & 1 + u_{2y}(x, y, t) & 0 \\ 0 & 0 & 1 \end{pmatrix}, \tag{3}$$

and $\mathbf{I}$ is the identity tensor. Thus, the in-plane strain of $\mathbf{E}$ can be expressed as

$$\begin{cases} E_{11} = u_{1x} + \frac{1}{2}u_{1x}^2 + \frac{1}{2}u_{2x}^2. \\ E_{22} = u_{2y} + \frac{1}{2}u_{1y}^2 + \frac{1}{2}u_{2y}^2. \\ E_{12} = E_{21} = \frac{1}{2}u_{1y} + \frac{1}{2}u_{1y}u_{1x} + \frac{1}{2}u_{2x} \\ \quad + \frac{1}{2}u_{2y}u_{2x}. \end{cases} \tag{4}$$

The second-, fourth- and sixth-order moments of the area about y-axis are used in the coming sections. These moments are

$$\int_A \mathrm{d}A = A, \quad \int_A y^2\mathrm{d}A = I,$$
$$\int_A y^4\mathrm{d}A = J, \quad \int_A y^6\mathrm{d}A = Q. \tag{5}$$

In order to develop an asymptotically consistent approximate model for the problem, the terms with fourth-

and sixth-order moments are neglected in the following derivations, and a justification for it is given in Remark 1.

The work done by the moving load P is given by

$$W = \int_0^L \int_A Pu_2(x, y, t)\delta(x - \gamma t)\mathrm{d}A\mathrm{d}x. \tag{6}$$

Substituting (1) into (6) and integrating the resulting equation over the cross section, it yields

$$W = \int_0^L P\left((w_0\delta(x - \gamma t) + \frac{I}{2}\nu w_{0xx}\delta(x - \gamma t))\right)\mathrm{d}x. \tag{7}$$

The kinetic energy T of the beam can be written as

$$T = \frac{1}{2}\rho \int_0^L \int_A (u_{1t}^2 + u_{2t}^2)\mathrm{d}x\mathrm{d}A. \tag{8}$$

By substituting (1) into (8) and integrating the resulting equation over the cross section, the following expression can be obtained

$$T = \frac{1}{2}\rho \int_0^L \left(Au_{0t}^2 + Aw_{0t}^2 \right. \\ \left. + I(\nu^2 u_{0xt}^2 + w_{0xt}^2 + \nu w_{0t}w_{0xxt})\right)\mathrm{d}x. \tag{9}$$

As can be seen from (7) and (9), there are some terms with coefficient ν which do not appear in most of the existing beam theories. Such terms imply that the effects of material parameter ν, the second-order moment I on the work done by the moving load and the kinetic energy of the beam are taken into account.

For two-dimensional isotropic linear materials, the total potential energy Φ of the beam is given by

$$\Phi = \int_0^L \int_A \mathbf{V}\mathrm{d}A\mathrm{d}x, \tag{10}$$

where

$$\mathbf{V} = \frac{1}{2}(S_{11}E_{11} + S_{22}E_{22} + 2S_{12}E_{12}), \tag{11}$$

and $S_{ij}(i = 1, 2; j = 1, 2)$ are the nominal (First Piola-Kirchhoff) stress tensors. As the cross-sectional boundary of the beam is free of surface traction, the plane stress assumption can be made. According to the generalized Hooke's law, the relations between the stress and strain are given by

$$\begin{cases} S_{11} = \dfrac{E}{(1-v_1^2)}\left(E_{11} + v_1 E_{22}\right), \\[2mm] S_{22} = \dfrac{E}{(1-v_1^2)}\left(v_1 E_{11} + E_{22}\right), \\[2mm] S_{12} = S_{21} = \dfrac{E}{(1+v_1)}E_{12}, \end{cases} \quad (12)$$

where E is Young's modulus and v_1 is Poisson's ratio. It should be pointed out that, in general, the range of Poisson's ratio is $-1 < v_1 < 0.5$. For some graphene materials, Poisson's ratio may fall within the range of $-1 < v_1 < 0$. As engineering solid material is considered in this paper, Poisson's ratio of common stable solid materials falls within the range of $0 < v_1 < 0.5$. In the calculations, Poisson's ratio v_1 is replaced by in-plane Poisson's ratio v through the relation

$$v_1 = \frac{v}{1+v}, \quad \text{or} \quad v = \frac{v_1}{1-v_1}, \quad (13)$$

from which one can also find that in-plane Poisson's ratio falls within the range of $0 < v < 1$.

By substituting (1), (11) and (12) into (10), after some further manipulations one can obtain the total potential energy Φ in terms of the displacements (refer to "Appendix B" for details).

Now, the governing equations in terms of the displacements for the vibration problem can be derived using the Hamilton principle

$$\delta \int_{t_1}^{t_2} (T - \Phi - W)\mathrm{d}t = 0. \quad (14)$$

The resulting approximate model equations are included in "Appendix B"; they are Eqs. (45) and (46).

By introducing some dimensionless parameters as follows

$$x = Lx^*, \quad u_0 = Lu^*, \quad w_0 = Lw^*, \quad t = \sqrt{\frac{E}{\rho L^2}}t^*,$$

$$p^* = \frac{P}{E}, \quad k_s = \frac{I}{AL^2}, \quad \gamma^* = \sqrt{\frac{E}{\rho L^4}}\gamma, \quad (15)$$

model Eqs. (45) and (46) can be rewritten as

$$\begin{cases} u_{tt} + a_1 u_{xx} + a_2 w_x w_{xx} + k_s(a_3 w_{xx} w_{xxx} \\ \quad + a_4 u_{xxxx} + a_5 w_x w_{xxxx} - v^2 u_{xxtt}) = 0, \\ w_{tt} + a_2(w_x u_{xx} + w_{xx} u_x) + a_6 w_x^2 w_{xx} \\ \quad + k_s\big(a_7 w_{xx}^3 + (v-1)w_{xxtt} + a_8 u_{xx} w_{xxx} \\ \quad + w_{xx}(a_9 u_{xxx} + 4a_7 w_x w_{xxx}) + a_5 w_x u_{xxxx} \\ \quad + \tfrac{1}{2}a_8 u_x w_{xxxx} + (-a_1 + a_7 w_x^2)w_{xxxx}\big) \\ \quad = p\delta(x - \gamma t) + \tfrac{1}{2}p k_s v \delta_{xx}(x - \gamma t), \end{cases} \quad (16)$$

where, for convenience, the superscript "$*$" has been removed, and the transformation of the Dirac delta function $\delta(x^* - \gamma^* t^*) = \frac{1}{l}\delta(x - \gamma t)$ has been used. The geometrical parameter k_s, for a beam with rectangular cross section, can be expressed as

$$k_s = \frac{I}{AL^2} = \frac{1}{12}\left(\frac{d}{L}\right)^2, \quad (17)$$

with d being the width of the cross section of the beam. Obviously, k_s is relatively small for a slender beam.

It is crucial to set up the boundary conditions for a model with finite deformation setting. For the simply supported boundary considered here, the conditions imposed on the nondimensionalized displacements can be expressed as

$$\begin{cases} u = 0, \quad u_{xx} = 0, \quad \text{at} \quad x = 0, 1, \\ w = 0, \quad w_{xx} = 0, \quad \text{at} \quad x = 0, 1. \end{cases} \quad (18)$$

The details of the derivations are shown in "Appendix B".

Compared with existing models in the literature, model Eq. (16) has four new features: (a) the finite deformation kinematics is adopted, where the effect of the second-order moment on the kinetic energy and total potential energy is taken into account. The effect is reflected by the terms with coefficient k_s, such as $k_s a_4 u_{xxxx}$, $\frac{1}{2}p k_s \delta_{xx}(x - \gamma t)$, $k_s a_3 w_{xx} w_{xxx}$ and so on. (b) The effect of the longitudinal vibration on the transverse vibration is represented, as indicated with the occurrence of the terms with coefficient v. (c) The total potential energy is established for the entire system as a result of the deformation of the beam. (d) The higher-order nonlinear terms of the longitudinal and transverse displacement are involved, whereas it is not usually the case for some existing models in which the nonlinear terms arise from the elastic foundation of the beam. Thus, it is expected that the present model can capture more features of nonlinear vibration of beams than existing models.

Remark 1 In developing approximate model Eq. (16), terms were only kept up to the second-order moment I, while terms associated with the fourth-order moment J, sixth-order moment Q and some other higher-order moments in Eqs. (9) and (43) ("Appendix B") were neglected. It can be shown that the contribution of J, Q and other higher-order moments are relatively small as compared with that of the second-order moment I. In fact, after nondimensionalization, J becomes $\frac{J}{AL^4}$, which means that $\frac{J}{AL^4} \sim (k_s)^2$ (c.f. (17)). Similarly, for the sixth-order moment Q, it leads to $\frac{Q}{AL^6} \sim (k_s)^3$. As k_s is relatively small for a slender beam, J, Q and other higher-order moments can be dropped to obtain an approximate model equation.

2.2 Simplified model equations

Model (16) is rather complex. In this subsection, a decoupled and simplified version of it shall be derived with appropriate assumptions. In [35], for transverse vibration of axially moving beams, the stretch of the beam was assumed to be quasi-static, and hence, the effect of velocity on longitudinal displacement was neglected. For the present problem, it is also reasonable to make similar assumptions. Thus, the fast dynamic terms in Eq. (16)$_1$ can be neglected ($u_{tt} = 0$). Furthermore, as geometrical parameter k_s is considered to be small, the related terms in Eq. (16)$_1$ can be neglected. Then, (16)$_1$ can be approximately written as

$$a_2 w_x w_{xx} + a_1 u_{xx} = 0. \tag{19}$$

With boundary conditions (18), Eq. (19) gives

$$u(x, t) = \frac{a_2 x}{2a_1} \int_0^1 w_s^2 ds - \frac{a_2}{2a_1} \int_0^x w_s^2 ds. \tag{20}$$

After substituting (20) into (16)$_2$, this yields a single equation for the transverse displacement as follows

$$w_{tt} + a_{10} w_x^2 w_{xx} + k_s \left(\left(a_7 - \frac{a_2 a_9}{a_1} \right) w_{xx}^3 + (v - 1) w_{xxtt} \right.$$
$$\left. + a_{11} w_x w_{xx} w_{xxx} - a_1 w_{xxxx} + a_{12} w_x^2 w_{xxxx} \right)$$
$$+ \left(\frac{a_2^2}{2a_1} w_{xx} + \frac{a_2 a_8}{4a_1} k_s w_{xxxx} \right) \int_0^1 w_x^2 dx$$
$$= p\delta(x - \gamma t) + \frac{1}{2} p k_s v \delta_{xx}(x - \gamma t), \tag{21}$$

where

$$\begin{cases} a_{10} = a_6 - \frac{3a_2^2}{2a_1}, \quad a_{11} = -\frac{3a_2 a_5}{a_1} \\ \quad + 4a_7 - \frac{a_2 a_8}{a_1} - \frac{a_2 a_9}{a_1}, \\ a_{12} = -\frac{a_2 a_5}{a_1} + a_7 - \frac{a_2 a_8}{4a_1}. \end{cases} \tag{22}$$

If the transverse displacement is relatively small, the nonlinear terms in (21) can be neglected to obtain the following linear equation

$$w_{tt} + k_s \left((v - 1) w_{xxtt} - a_1 w_{xxxx} \right)$$
$$= p\delta(x - \gamma t) + \frac{1}{2} p k_s v \delta_{xx}(x - \gamma t). \tag{23}$$

If $v = 0$, (21) reduces to the following higher-order nonlinear equation

$$w_{tt} - \frac{3}{2} w_x^2 w_{xx} + k_s \Big(-2w_{xx}^3 - w_{xxtt}$$
$$-5w_x w_{xx} w_{xxx} + w_{xxxx} - \frac{1}{2} w_x^2 w_{xxxx} \Big)$$
$$- \left(\frac{1}{2} w_{xx} - \frac{3}{2} k_s w_{xxxx} \right) \int_0^1 w_x^2 dx$$
$$= p\delta(x - \gamma t). \tag{24}$$

Equation (24) can be viewed as a model equation for the vibration problem which considers the effect of finite deformation based on Euler–Bernoulli beam theory. Further, if the nonlinear terms in (24) are neglected, it then reduces to the following equation

$$w_{tt} + k_s \left(-w_{xxtt} + w_{xxxx} \right) = p\delta(x - \gamma t), \tag{25}$$

which can be viewed as a linear model derived on the basis of finite deformation and Euler–Bernoulli beam theory.

2.3 Model equations based on Euler beam theory

In this subsection, the model equation is reformulated using Euler beam theory [i.e., material parameter $v = 0$ in Eq. (1)] based on small deformation assumption. The superscript E in the following formulae denotes the corresponding quantity in Euler beam theory.

The work W^E done by the moving load P, the kinetic energy T^E and the total potential energy Φ^E of the beam can be given, respectively, by

$$W^E = \int_0^L \int_A P w_0 \delta(x - \gamma t) dA dx, \tag{26}$$

$$T^E = \frac{1}{2} \rho \int_0^L \int_A \left(u_{0t}^2 + w_{0t}^2 \right) dA dx. \tag{27}$$

and

$$\Phi^E = \frac{1}{2} \int_0^L \int_A \mathbf{e}_{xx}^E \sigma_{xx}^E \mathrm{d}A \mathrm{d}x, \tag{28}$$

with

$$\mathbf{e}_{xx}^E = u_{0x} + \frac{1}{2} w_{0x}^2, \quad \sigma_{xx}^E = E \mathbf{e}_{xx}^E. \tag{29}$$

With a similar method as described in Sect. 2.2, the model equation of the vibration for a Euler beam under a moving load can be obtained as

$$w_{tt} + k_s w_{xxxx} - \frac{1}{2} w_{xx} \int_0^1 w_x^2 \mathrm{d}x = p\delta(x - \gamma t). \tag{30}$$

If the nonlinear terms in (30) are dropped, it becomes

$$k_s w_{xxxx} + w_{tt} = p\delta(x - \gamma t), \tag{31}$$

which is the classical linear model equation for a Euler beam under a moving load.

It is to be noted that, as compared with Euler beam model (31), an additional term w_{xxtt} appears in (25). Such a discrepancy can be interpreted as: The effect of finite deformation is taken into account in the novel formulation (24), while such an effect is neglected in the Euler beam model. In other words, the Euler beam model (30) is based on the small deformation formulation.

3 Numerical solutions and discussions

In this section, the Galerkin method is used to solve integro-differential Eqs. (21) and (30) presented in Sect. 2, and then, some discussions for various models will be made.

According to boundary condition (18) and the Fourier harmonics, the asymptotic solution to $w(x, t)$ can be expressed as

$$w(x, t) = \sum_{i=1}^N p_i(t)\phi_i(x), \tag{32}$$

where $\phi(x) = \sin(i\pi x)(i = 1, 2, \ldots N)$ are the linear fundamental vibration modes and $p_i(t)$ denotes the ith generalized coordinate for the transverse motion.

As to model (21), after substituting (32) into (21) and applying the Galerkin method, it can be transformed into the nonlinear ordinary differential Eq. (33).

$$\sum_{i=1}^N \left(\int_0^1 \phi_i \phi_j dx \right) p_{itt}$$

$$+ a_{10} \sum_{i=1}^N \sum_{l=1}^N \sum_{k=1}^N \left(\int_0^1 \phi_{ix}\phi_{lx}\phi_{kxx}\phi_j dx \right) p_i p_l p_k$$

$$+ k_s \left[\left(a_7 - \frac{a_2 a_9}{a_1} \right) \sum_{i=1}^N \sum_{k=1}^N \sum_{l=1}^N \right.$$

$$\times \left(\int_0^1 \phi_{kxx}\phi_{ixx}\phi_{lxx}\phi_j dx \right) p_i p_k p_l + (\nu - 1)$$

$$\times \sum_{i=1}^N \left(\int_0^1 \phi_{ixx}\phi_j dx \right) p_{itt}$$

$$+ a_{11} \sum_{i=1}^N \sum_{l=1}^N \sum_{k=1}^N \left(\int_0^1 \phi_{kx}\phi_{ixx}\phi_{lxxxx}\phi_j dx \right) p_i p_k p_l$$

$$- a_1 \sum_{i=1}^N \left(\int_0^1 \phi_{ixxxx}\phi_j dx \right) p_i$$

$$+ a_{12} \sum_{i=1}^N \sum_{l=1}^N \sum_{k=1}^N \left(\int_0^1 \phi_{kx}\phi_{ix}\phi_{lxxxx}\phi_j dx \right) p_i p_k q_l \right]$$

$$+ \int_0^1 \left(\sum_{i=1}^N \sum_{k=1}^N \phi_{ix}\phi_{kx} p_i p_k \right) dx$$

$$\times \left[\frac{a_2^2}{2a_1} \sum_{i=1}^N \left(\int_0^1 \phi_{ixx}\phi_j dx \right) p_i \right.$$

$$+ \frac{a_2}{4a_1} a_8 k_s \sum_{i=1}^N \left(\int_0^1 \phi_{ixxxx}\phi_j dx \right) p_i \right]$$

$$= p \sin(j\pi\gamma t) - \frac{1}{2}\nu p k_s j^2 \pi^2 \sin(j\pi\gamma t),$$
$$j = 1, 2, \ldots N, \tag{33}$$

In the derivations, the following formulae concerning δ function are used

$$\int_0^1 f(x)\delta(x - x_0)dx = f(x_0),$$

$$\int_0^1 f(x)\delta_{xx}(x - x_0)dx = f_{xx}(x_0), \tag{34}$$

with $f(x)$ being an arbitrary function.

In this paper, (33) is solved numerically using a direct time integration by the variable step-size Runge–Kutta method. For simplicity, $N = 8$ is used in the calculations. The initial conditions are

$$p_i(0) = 0, \quad p_{it}(0) = 0, \quad i = 1, 2, \ldots 8. \tag{35}$$
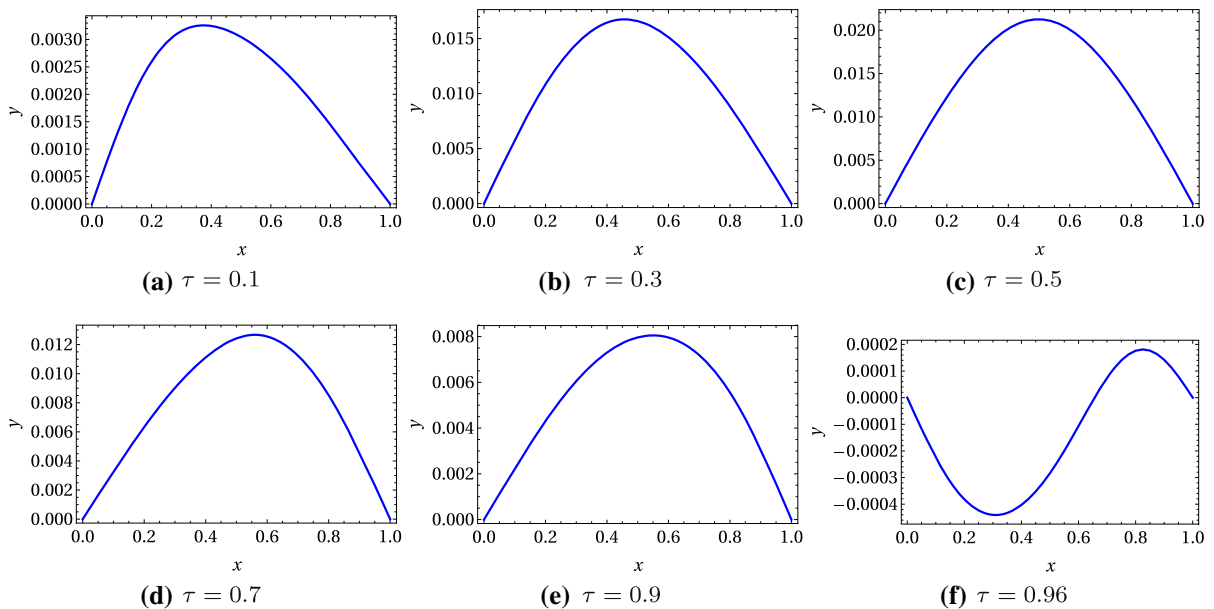
Fig. 1 The buckled configurations of the neutral axis of the beam in forced vibration at different time instants for $p = 0.01$, $v = 0.5$, $\gamma = 0.05$ and $k_s = 0.01$

The vibration amplitude of the beam is defined as the displacement of the beam center $w(0.5, t)$, which is given by

$$w(0.5, t) = p_1(t) - p_3(t) + p_5(t) - p_7(t). \quad (36)$$

It is the same case for (30), which is omitted for brevity. It should be mentioned that the dimensionless time $\tau = \gamma t$ is used in the following discussions. Thus, if $\tau \in [0, 1]$, then the beam is in the forced vibration state, while $\tau > 1$ means that the load leaves the beam.

3.1 Analysis of the solutions to the new model

In this subsection, the nonlinear dynamic response of the beam based on nonlinear model (21) will be analyzed.

With the numerical solutions obtained, the shape of the neutral line of the beam in forced vibration is plotted for some time instants in Fig. 1. As verification for the truncation in model Eq. (43) in "Appendix B", Fig. 2 shows some typical solutions for the vibration of the midpoint of the beam with given parameters. It can be seen that the longitudinal displacement is much smaller than the transverse displacement. A closer examination provides the following approximate relation

$$u(x, t) = O(w(x, t)^2). \quad (37)$$

Effect of the parameters

The effects of the material parameter v, geometrical parameter k_s and γ on the dynamic response of (21) are shown in Figs. 3, 4 and 5.

Figure 3 shows that in the forced vibration, the vibration amplitude decreases with the increase in the material parameter v, while in the free vibration such correlation becomes ambiguous. The reason may be that the amplitude of the free vibration also depends on the amplitude as the point load leaves the beam. Also, it can be seen from Fig. 3 that, as v increases, the fluctuation of the forced vibration becomes faster and the frequency of the free vibration increases. It should be pointed out that in the open literature, there are very few results for the effect of the material parameter.

As can be seen from Fig. 4, in the forced vibration the geometrical parameter k_s reduces the vibration amplitude. However, due to different initial amplitudes, this effect is not obvious in the free vibration state. Furthermore, as k_s increases, the fluctuation of the forced vibration becomes faster and the frequency of the free vibration increases. It seems that k_s plays a similar role as v in the dynamic response.

Fig. 2 Nonlinear vibration of the midpoint of the beam for $v = 0.5$, $k_s = 0.005$ and $\gamma = 0.05$. The blue and red solid lines denote the amplitude for $p = 0.02$ and $p = 0.01$, respectively. (Color figure online)
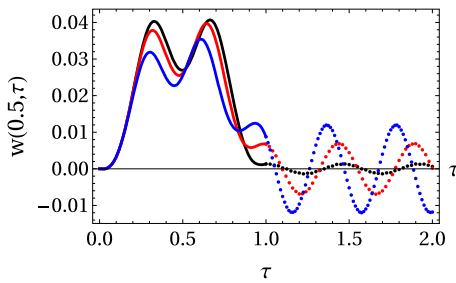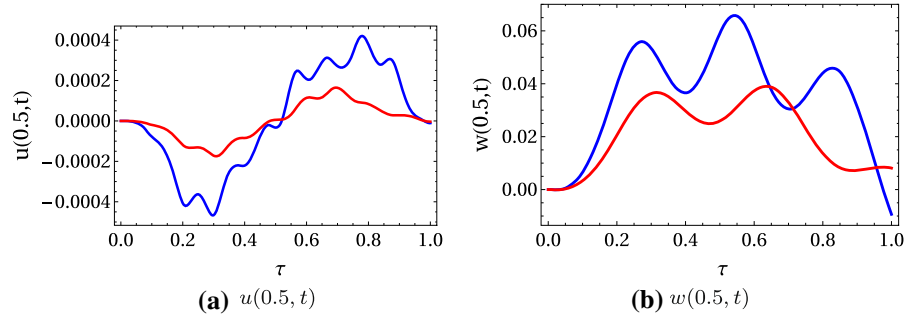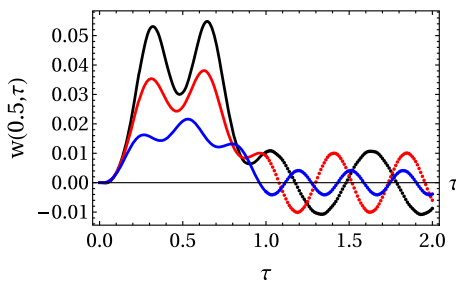

(a) $u(0.5, t)$

(b) $w(0.5, t)$

Fig. 3 The effect of v on the dynamic response of the beam for $p = 0.01$, $\gamma = 0.05$ and $k_s = 0.005$. The black, red and blue lines denote the results for $v = 0.1, 0.4$ and 0.8, respectively. Solid line: forced vibration, dotted line: free vibration. (Color figure online)
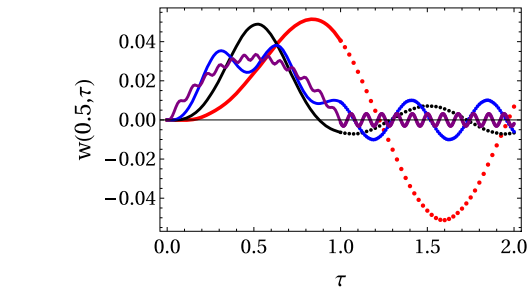

Fig. 5 The effect of γ on the dynamic response of the beam for $p = 0.01$, $v = 0.6$ and $k_s = 0.005$. The purple, blue, black and red lines denote the results for $\gamma = 0.01, 0.05, 0.1$ and 0.2, respectively. Solid line: forced vibration, dotted line: free vibration. (Color figure online)

Fig. 4 The effect of k_s on the dynamic response of the beam for $p = 0.01$, $\gamma = 0.05$ and $v = 0.6$. The black, red and blue lines denote the results for $k_s = 0.0025, 0.005$ and 0.01, respectively. Solid line: forced vibration, dotted line: free vibration. (Color figure online)

Figure 5 shows that, as γ increases, the fluctuation of the forced vibration becomes slow and the frequency of the free vibration decreases. The effect of γ on the amplitude of forced vibration is shown in Fig. 6. As can be seen from the figure, there is a value γ_c: If $\gamma < \gamma_c$, the maximum vibration amplitude (corresponding to each γ) gradually increases and reaches a maximum value

with the increase of γ. Otherwise, if $\gamma > \gamma_c$, the maximum vibration amplitude decreases with the increase of γ. Thus, γ plays an important role in determining the dynamic response. The numerical experiments (not included) also show that, when γ increases, the amplitude of the forced vibration decreases. As this continues, the amplitude becomes very small and almost independent of the parameters v and k_s.

Critical velocity

In the literature, for beams under moving loads, critical velocity has different meanings. Many articles such as [21–23] call the velocity which leads to the largest amplitude for the beam as the critical velocity. Thus, the critical value γ_c described above falls into this category. It can be obtained numerically, and the effect of the parameters k_s and v on γ_c is shown in Fig. 7. It is found that γ_c increases with the growth of k_s and v.

Another kind of critical velocity is described in [2]. It corresponds to the velocity which leads to the resonance phenomenon. Assuming that the moving load only induces a harmonic excitation with the frequency equaling a natural frequency of the beam, then accord-

Fig. 6 The curve of the maximum amplitude of forced vibration versus γ based on model Eq. (21) with $p = 0.01$. **a** The blue, red and black lines denote the results for $k_s = 0.005$, 0.01, and 0.02, respectively. **b** The blue, red and black lines denote the results for $\nu = 0.25$, 0.5 and 0.75, respectively. (Color figure online)
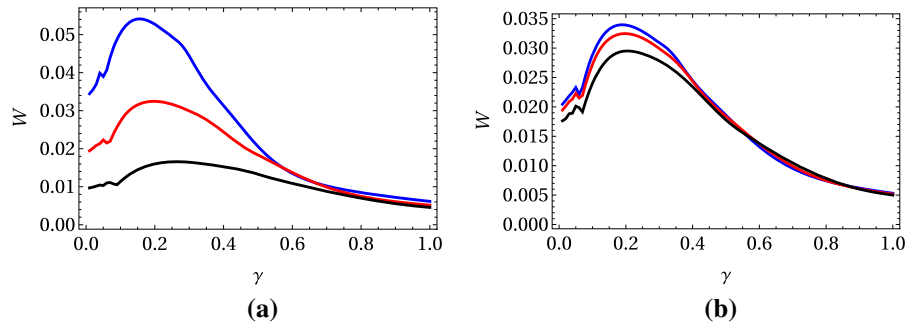

(a)   **(b)**

Fig. 7 The curve of the critical velocity γ_c versus the parameters based on Eq. (21). **a** The black, red and blue lines denote the results for $k_s = 0.02$, 0.01 and 0.005, respectively. **b** The black, red and blue lines denote the results for $\nu = 0.9$, 0.5 and 0.1, respectively. (Color figure online)
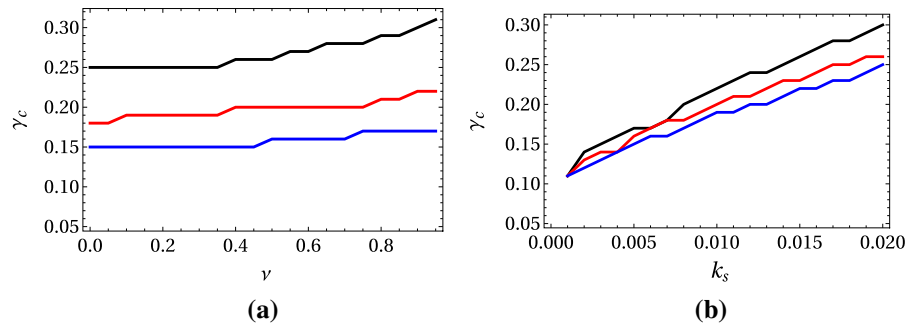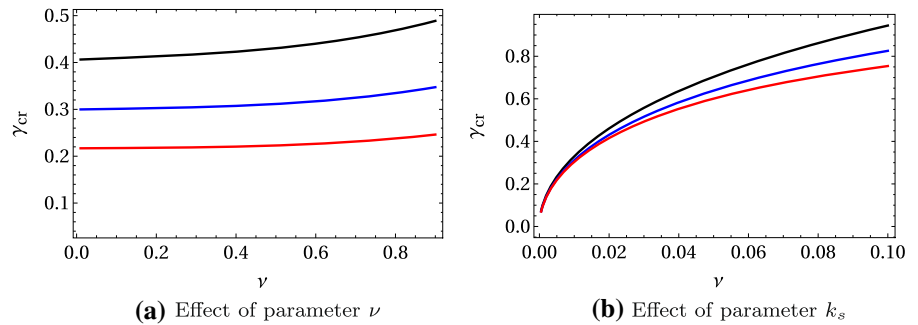

(a)   **(b)**

Fig. 8 The critical velocity γ_{cr} based on Eq. (38). **a** The black, blue and red lines denote the results for $k_s = 0.02$, 0.01 and 0.005, respectively. **b** The black, blue and red lines denote the results for $\nu = 0.75$, 0.5 and 0.25, respectively. (Color figure online)

(a) Effect of parameter ν **(b)** Effect of parameter k_s

ing to Eq. (33), the critical velocity in model (21) can be obtained as

$$\gamma_{cr} = \frac{\Omega_1}{\pi}, \tag{38}$$

where Ω_1 is the first natural frequency of the beam. According to Eq. (38), the effect of k_s and ν on γ_{cr} is shown in Fig. 8. The results indicate that γ_{cr} also increases with the growth of k_s and ν. Furthermore, it can be found from Figs. 7) and 8 that γ_c is less than γ_{cr}. It should be pointed out that γ_{cr} obtained in (38) only induces a single-mode resonance, whereas the critical velocity may induce a combination of resonances in general.

3.2 Comparison between the nonlinear and linear models

To reveal the nonlinear effect, the solution to nonlinear model (21) is compared with that of the corresponding linear model (23). These results are shown in Figs. 9, 10 and 11.

Figure (9) shows that, in the forced vibration, the vibration amplitude of linear model (23) is generally larger than that of the nonlinear model, and the discrepancy becomes smaller as p decreases. When $p = 0.001$, they are almost identical as shown in Fig. 9d. Furthermore, the decrease in p reduces not

Fig. 9 The vibration amplitude of the beam for different values of the point load, with $\nu = 0.5$, $k_s = 0.005$ and $\gamma = 0.05$ (fixed). Solid line: nonlinear model (21), dotted line: linear model (23)
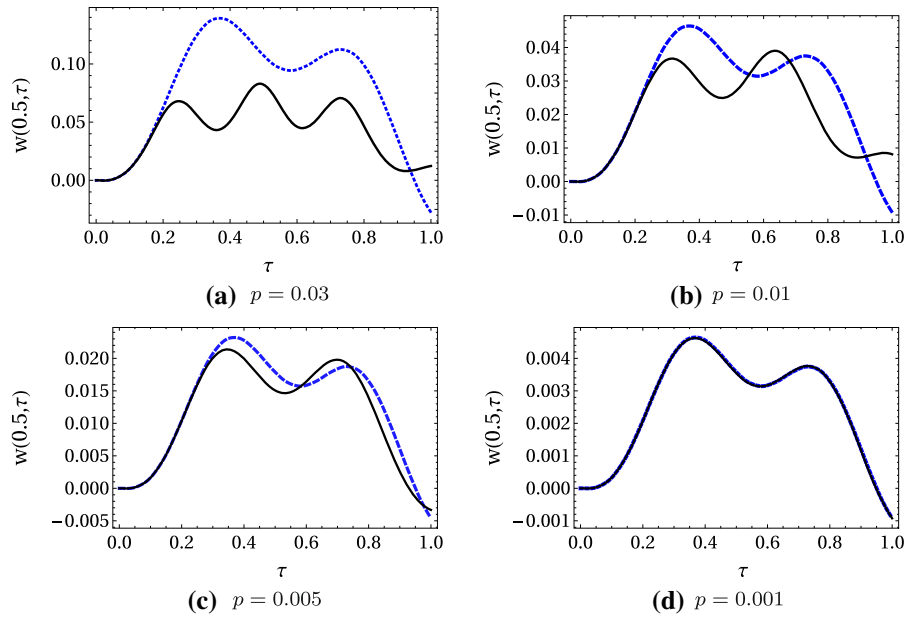

(a) $p = 0.03$

(b) $p = 0.01$

(c) $p = 0.005$

(d) $p = 0.001$

Fig. 10 The vibration amplitude of the beam in both forced and free vibration states, with $p = 0.01$, $\gamma = 0.05$ and $k_s = 0.005$ (fixed). Blue line: nonlinear model (21), black line: linear model (23). (Color figure online)
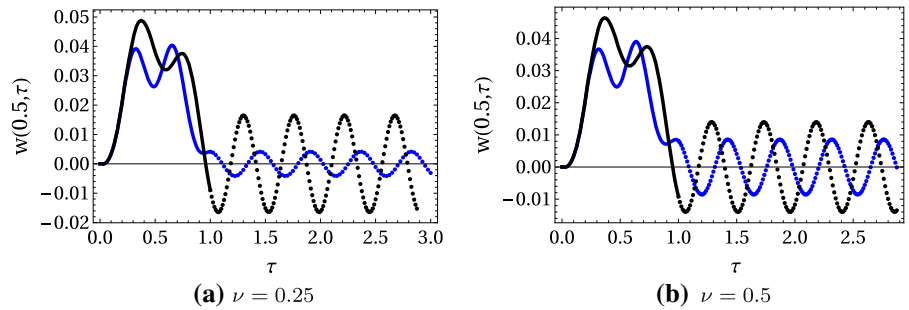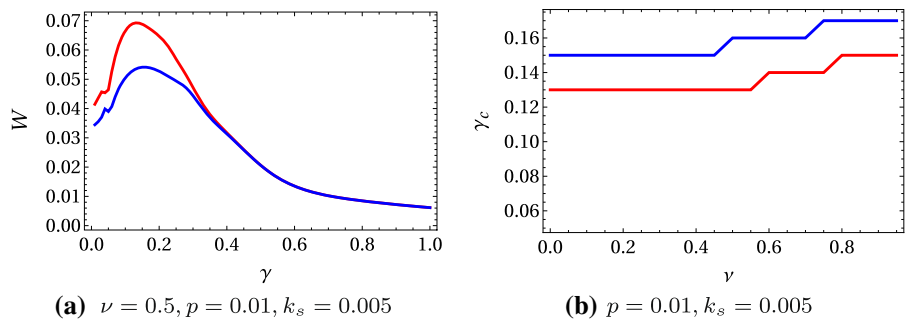

(a) $\nu = 0.25$

(b) $\nu = 0.5$

Fig. 11 **a** The effect of γ on the maximum vibration amplitude of the beam; **b** the effect of the material parameter ν on the critical velocity γ_c. Blue line: nonlinear model (21), red line: linear model (23). (Color figure online)

(a) $\nu = 0.5$, $p = 0.01$, $k_s = 0.005$

(b) $p = 0.01$, $k_s = 0.005$

only the transverse displacement $w(x, t)$ but also the fluctuations of the two models. Additionally, some further numerical experiments show that, if the geometrical parameter k_s is large enough, the dynamic response of the nonlinear model is similar to that of the linear model. In the free vibration state, Fig. 10 shows that

the relation between the vibration amplitudes of the two models is ambiguous, as they are both dependent on the initial values. Generally speaking, the nonlinear effect in (21) reduces the vibration amplitude and speeds up the fluctuation in the forced vibration. When the transverse displacement $w(x, t)$ is small, linear model (23)

Fig. 12 The vibration amplitude of the beam with $k_s = 0.005$ and $\gamma = 0.02$ (fixed). Solid line: model (24), dotted line: model (30)
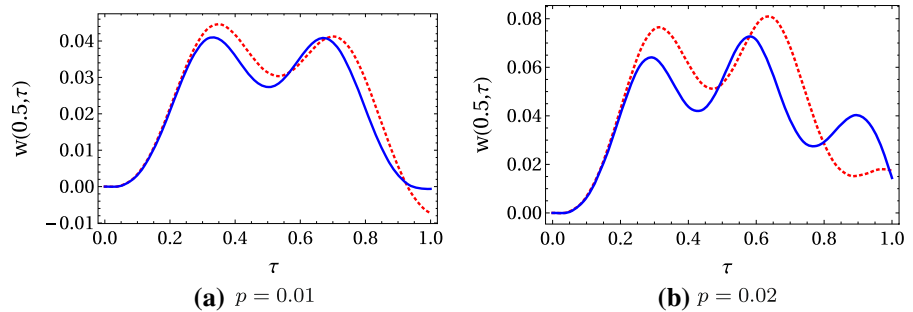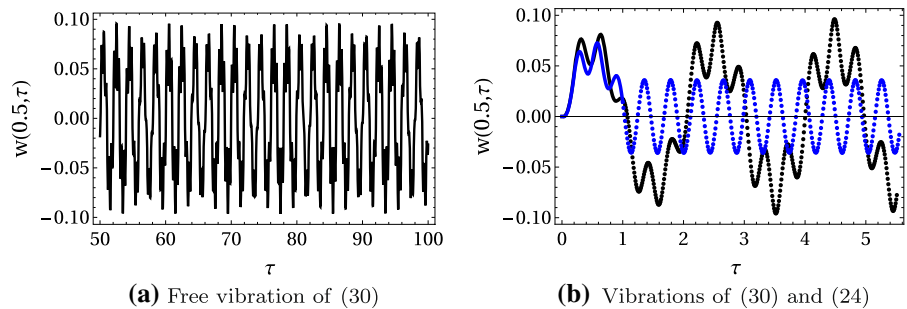

(a) $p = 0.01$

(b) $p = 0.02$

Fig. 13 For $p = 0.02$, $k_s = 0.005$ and $\gamma = 0.05$, **a** the free vibration of the Euler beam model (30), **b** the forced and free vibrations of models (24) and (30). Blue line: model (24), black line: model (30). (Color figure online)

(a) Free vibration of (30)

(b) Vibrations of (30) and (24)

is capable of capturing the main features of the dynamic response.

Figure 11a shows that the difference between the maximum vibration amplitudes (corresponding to a given γ) of the nonlinear and linear models firstly increases with the growth of γ. Subsequently, after reaching a maximum it decreases with the increase of γ. Figure 11b shows that the critical velocity γ_c of linear model (23) is less than that of nonlinear model (21). Moreover, it can be found that if the material parameter ν is small, then γ_c for the two models is almost independent of ν.

3.3 Comparison with the Euler beam model: the effect of finite deformation

To investigate the effect of finite deformation on the vibration of the beam, the dynamic response of finite deformation-based model (24) and small deformation-based Euler beam model (30) are compared. It is to be noted that their corresponding linear models are Eqs. (25) and (31), respectively.

Figure 12 shows that, even for small values of p, the vibration amplitude of (24) is smaller than that of (30) in the forced vibration state. It is expected that the

difference becomes larger with the growth of the load p. According to Fig. 13a, the free vibration of the midpoint of the Euler beam (30) is not a harmonic vibration, while Fig. 13b shows that the free vibration of (24) is a harmonic one. The above-mentioned differences result from the different calculations for the strain in the two models. It also implies that finite deformation does play an important role in determining the dynamic response.

In order to compare the response of the beam when the point load moves at or near the critical velocity γ_{cr} [c.f. (38)], it is necessary to firstly calculate and compare the natural frequency of the novel formulation (21) with that of Euler beam model (31). The natural frequency of these two models can be easily determined as

$$\omega = \frac{k^2\pi^2(1+\nu)\sqrt{k_s}}{\sqrt{\left(1 + k^2\pi^2(1-\nu)k_s\right)(1+2\nu)}}$$
$$\omega^E = k^2\pi^2\sqrt{k_s}, k = 1, 2, \ldots. \tag{39}$$

The effects of the material parameter ν and geometrical parameter k_s on the natural frequency are plotted in Fig. 14. In Fig. 14a, the results show that the natural frequency ω increases with the increase of ν, and it exceeds ω^E when ν is large enough. Furthermore, the difference between ω and ω^E becomes larger with the growth of wave number k. Similar conclusions can be

Fig. 14 The effect of the parameters on the natural frequency of the beam. **a** The effect of ν, with $k_s = 0.008$; **b** the effect of k_s, with $\nu = 0.5$. Solid line: nonlinear model (21), dotted line: Euler beam model (31). The red, blue and black lines in each case denote the results for wave numbers $k = 1$, 2 and 3, respectively. (Color figure online)
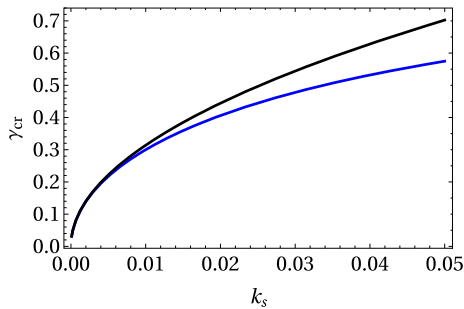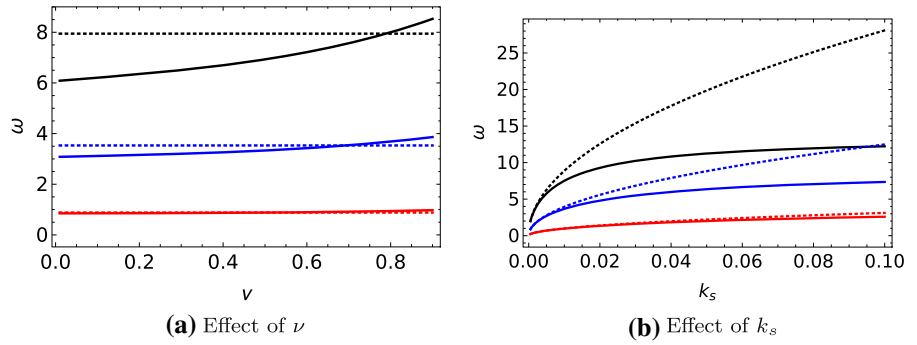
(a) Effect of ν

(b) Effect of k_s

Fig. 15 The effect of k_s on the critical velocity γ_{cr} with $p = 0.01$. Blue line: model (25), black line: model (31). (Color figure online)

drawn for the effect of k_s (Fig. 14b). The natural frequency for model (24) or (25) can be obtained by setting $\nu = 0$ in (39)$_1$. Based on (38) and (39), the curves of γ_{cr} for the corresponding linear models (25) and (31) are plotted in Fig. 15. It shows that, for small values of k_s, the critical velocity γ_{cr} of (25) is almost identical to that of (31). However, the difference becomes larger with the growth of k_s.

The following comparisons between the models are made when the point load moves at or near the critical velocity γ_{cr}, with $p = 0.01$ fixed.

Letting $k_s = 0.001$, the values of γ_{cr} for (24) and (30) can be obtained as 0.0988592 and 0.0993459, which are very similar. The corresponding curves of the forced vibration with $\gamma = 0.0988592$ for (24), (30) and their linear counterparts (25), (31) are plotted in Fig. 16a. It shows that, as the point load moves at the critical velocity, the vibration amplitude of (24) is smaller than (30). Interestingly, the dynamic response of (25) and (31) are almost identical.

Letting $k_s = 0.015$, the value of γ_{cr} for (24) and (30) is then 0.359101 and 0.384765, respectively. Figure 16b shows the dynamic response of models (24), (25), (30) and (31) when $\gamma_{cr} = 0.359101$. It can be

seen that, for a larger value of k_s, the dynamic responses of the small deformation-based models (30) and (31) become closer to the finite deformation-based models (24) and (25). Figure 16c shows the dynamic responses of (24) and (25) with $\gamma = 0.359101$, and also the dynamic response of (30) and (31) with $\gamma = 0.384765$. It is found that the four curves are almost the same. In fact, if k_s is appropriately large, the dynamic response of the former models with $\gamma = \gamma_{cr}$ is identical to that of the latter models.

Letting $k_s = 0.002$ and $k_s = 0.018$ in turn, the critical velocity γ_{cr} is 0.13913 and 0.388398, respectively. Figure 17 shows the response of the beam when the point load moves at a speed γ which is close to γ_{cr}. It is found that, similarly to the case where $\gamma = \gamma_{cr}$, the vibration amplitude of (24) is less than that of (30), and this discrepancy becomes smaller as k_s increases.

To summarize, the finite deformation-based model predicts a smaller vibration amplitude than the small deformation-based model regardless of the velocity of the moving load, and this difference becomes smaller as k_s gets larger.

4 Conclusions

In this paper, with a recently developed kinematic frame, the vibration of a beam under a moving load is investigated in the finite deformation setting. The effects of both the material and geometrical parameters on the dynamic response are examined thoroughly, and comparisons are also made with the Euler beam model. The following conclusions can be drawn:

(1) Both the in-plane Poisson's ratio and geometrical parameter reduce the amplitude of the forced vibration, increase the speed of the fluctuation and increase the critical velocity (both γ_c and γ_{cr}).

Fig. 16 Dynamic responses of the beam with $\gamma = \gamma_{cr}$. Blue solid line: (24), blue dotted line: (24), red solid line: (30), red dotted line: (31). (Color figure online)
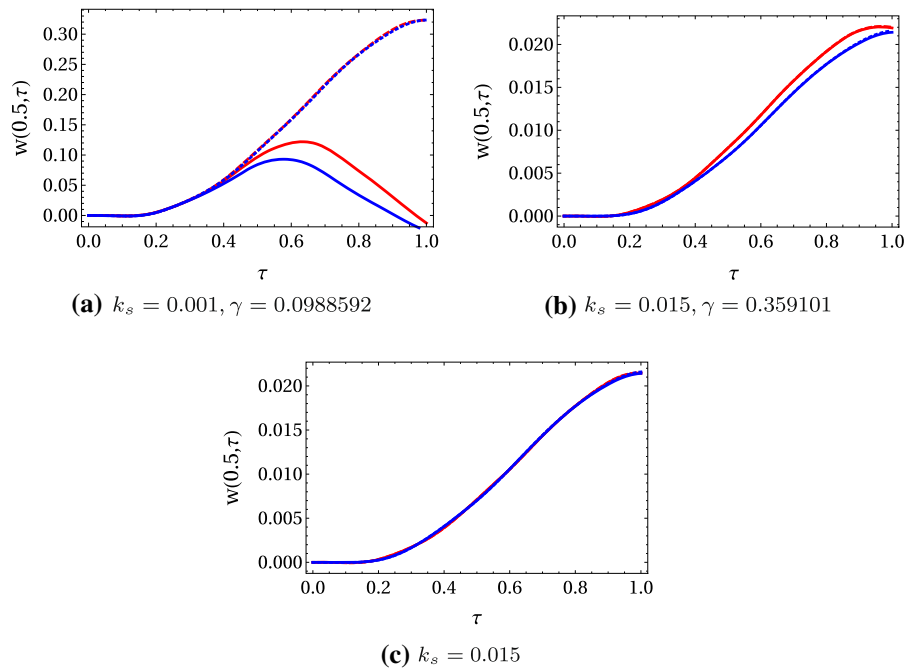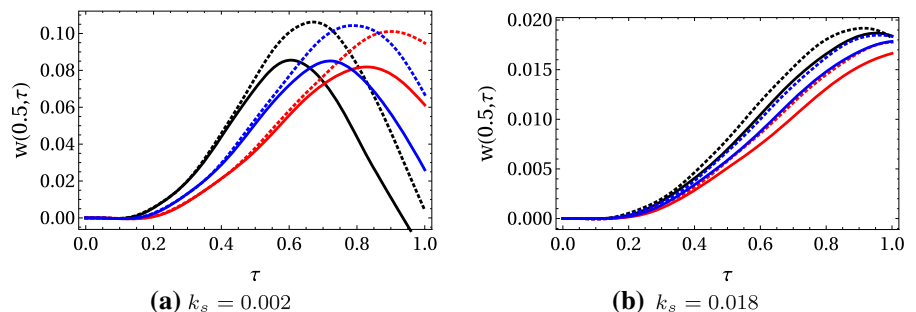

(a) $k_s = 0.001, \gamma = 0.0988592$

(b) $k_s = 0.015, \gamma = 0.359101$

(c) $k_s = 0.015$

Fig. 17 Dynamic responses of (24) (in solid line) and (30) (in dotted line) when γ takes values near γ_{cr}. **a** The blue, red and black lines denote the results for $\gamma = 0.13913, 0.16913$ and 0.10913, respectively; **b** the blue, red and black lines denote the results for $\gamma = 0.388398, 0.428398$ and 0.34839, respectively. (Color figure online)

(a) $k_s = 0.002$

(b) $k_s = 0.018$

(2) If the vibration amplitude is relatively small, higher-order linear model (23) may be used instead of nonlinear model (21) while preserving the main features.

(3) As compared with small deformation formulations, the effect of finite deformation herein is to reduce the vibration amplitude, especially for slender beams.

In summary, the present model can capture more features of the point load-induced vibration problem, especially for slender beams undergo large deformations. In future work, it can be applied to study nonlinear vibration of beams under moving loads or mass with nonlinear foundations.

Appendix A

Some details about kinematic frame (1) is presented in this "Appendix". The notations have the same meanings as they are in the main body.

Assuming that u_1, u_2 are sufficiently smooth in y, as y is a small variable for a beam structure, the Taylor series expansions in the neighborhood of $y = 0$ read

$$\begin{cases} u_1(x,y,t) = u_0(x,t) + yu_{10}(x,t) + \cdots, \\ u_2(x,y,t) = w_0(x,t) + yw_{10}(x,t) \\ \quad + y^2 w_{20}(x,t) + \cdots. \end{cases} \tag{40}$$

Since the transverse displacement is a key factor in the deformation, u_2 is expanded up to the second order of y in the derivation. Substituting Eq. (40) into the field equation of the beam and by the vanishing of each power of y, the relations among u_{10}, w_{10} and w_{20} can be obtained, after which (40) can be rewritten as (1). It should be pointed out that such a procedure is similar to the method presented in [36–38], and the parameter v can also determined as [33].

In Eq. (1)$_2$, the second term u_{0x} implies that the effect of the axial strain on the transverse displacement is taken into account, and the third term w_{0xx} (curvature of the beam due to shear) means that shear deformation is taken into account [39,40].

After deformation, the slope of the tangent line of the cross section is given by

$$k = -\frac{1 - vu_{0x} + yvw_{0xx}}{w_x}, \tag{41}$$

which means that the cross section in the deformed beam does not remain planar due to shear deformation. If the shear deformation is neglected, the slope reduces to

$$k = -\frac{1 - vu_{0x}}{w_x}, \tag{42}$$

which implies that the cross section of the beam remains planar. In Timoshenko beam and Reddy beam theories, the cross section of the beam remains planar. However, in the present formulation (1) the cross-sectional warps after deformation. Furthermore, as compared with Timoshenko beam and Reddy beam theories, the present formulation (1) can well capture the homogenous deformation of the beam under axial load.

Appendix B

This "Appendix" includes some details of the derivation of the model equations as well as the boundary conditions for the vibration problem.

Substituting (7), (9) and (10) into (14), after integration by parts and some manipulations, the corresponding equation which keeps terms up to the second-order moment I can be obtained. The resulting equation is intractable, and its lengthy expressions are omitted for

brevity. To further approximate this equation and get a model consistently in the order of the displacements, it is important to note that $u(x,t)$ is much smaller than $w(x,t)$, and to be more precise, $u(x,t) \sim O(w(x,t)^2)$. This can be confirmed from the numerical solutions in Fig. 2. Thus, to be consistent, the transverse and longitudinal displacements in the aforementioned equation are kept up to the fourth order and second order, respectively. To summarize, for a slender beam, the variational equation with accuracy to the fourth order of the transverse displacement can be achieved, which is shown in (43).

$$\begin{aligned}
&\int_0^L \int_{t_1}^{t_2} \Bigg(A\rho u_{0tt} + AE\big(a_1 u_{0xx} + a_2 w_{0x} w_{0xx} \\
&\quad - I\rho v^2 u_{0xtt}\big) \\
&\quad + EI\big(a_3 w_{0xx} w_{0xxx} + a_4 u_{0xxxx} \\
&\quad + a_5 w_{0x} w_{0xxxx}\big)\Bigg)\delta u_0 \, dx \, dt \\
&+ \int_0^L \int_{t_1}^{t_2} \Bigg(AP\delta(x - t\gamma) + \frac{1}{2} I P v \delta_{xx}(x - \gamma t) \\
&\quad + A\rho w_{0tt} \\
&\quad + AE\big(a_2 w_{0x} u_{0xx} + a_2 u_{0x} w_{0xx} + a_6 w_{0x}^2 w_{0xx}\big) \\
&\quad + I\rho(v-1)w_{0xtt} + EI\big(a_7 w_{0xx}^3 \\
&\quad + a_8 u_{0xx} w_{0xxx} + a_9 u_{0xxx} w_{0xx} \\
&\quad + 4a_7 w_{0x} w_{0xx} w_{0xxx} + a_5 w_{0x} u_{0xxxx} \\
&\quad + \frac{1}{2} a_8 u_{0x} w_{0xxxx} \\
&\quad - a_1 w_{0xxxx} + a_7 w_{0x}^2 w_{0xxxx}\big)\Bigg)\delta w_0 \, dx \, dt \\
&+ \int_0^L \Bigg(-A\rho\big(u_{0t}^2 \delta u_0|_{t_1}^{t_2} + w_{0t}^2 \delta w_0|_{t_1}^{t_2}\big) \\
&\quad - I\rho v^2 u_{0tx} \delta u_{0x}|_{t_1}^{t_2} \\
&\quad - I\rho w_{tx} \delta w_{0x}|_{t_1}^{t_2} - \frac{1}{2} I\rho v w_{0xxt} \delta w_0|_{t_1}^{t_2} \\
&\quad - \frac{1}{2} I\rho v w_{0t} \delta w_{0xx}|_{t_1}^{t_2}\Bigg) dx \\
&+ \int_{t_1}^{t_2} \Bigg(AE\big(b_1 w_{0x} u_{0x} + 4b_2 w_{0x}^3\big) \\
&\quad + I\rho\big(w_{ttx} - \frac{1}{2} v w_{0xxt} - \frac{1}{2} v w_{0ttx}\big) \\
&\quad + EI\big(vb_1 w_{0xx} u_{0xx} - vb_1\big(w_{0xx} u_{0xx} + w_{0x} u_{0xxx}\big) \\
&\quad - 2b_3 w_{0xxx} - 2b_5 w_{0xxx} w_{0x}^2 - 2b_5 w_{0xx}^2 w_{0x} \\
&\quad + 6vb_2 w_{0x}^2 w_{0xxx} \\
&\quad + 6vb_2 w_{0xx}^2 w_{0x} - 2b_6\big(w_{0xxx} u_{0x} + w_{0xx} u_{0xx}\big)
\end{aligned}$$

$$+ \frac{1}{2} v b_1 u_{0x} w_{0xxx}$$
$$+ \frac{1}{2} (u_{0xxx} w_{0x} + 2 u_{0xx} w_{0xx} + u_{0x} w_{0xxx}))$$
$$- \frac{1}{2} I P v \delta_x (x - \gamma t) \Big) \delta w_0 |_0^L \mathrm{d}t$$
$$+ \int_{t_0}^{t_1} \Big(AE(b_1 w_{0x}^2 + b_3 u_{0x}) + I \rho v^2 u_{0ttx}$$
$$- EI(2 b_4 u_{0xxx} + v b_1 (w_{0xx}^2 + w_{0x} w_{0xxx})$$
$$- b_6 w_{0xx}^2 - \frac{1}{2} v b_1 w_{0x} w_{0xxx}) \Big) \delta u_0 |_0^L \mathrm{d}t$$
$$+ \int_{t_1}^{t_2} \Big(EI(v b_1 w_{0x} u_{0xx} + 2 b_3 w_{0xx}$$
$$- 3 b_2 v w_{0x}^2 w_{0xx} + 2 b_5 w_{0x}^2 w_{0xx})$$
$$+ EI(2 b_6 w_{0xx} u_{0x}$$
$$- \frac{1}{2} v b_1 (u_{0xx} w_{0x} + u_{0x} w_{0xx})) \Big) \delta w_{0x} |_0^L \mathrm{d}t$$
$$+ \int_{t_1}^{t_2} \Big(EI(2 b_4 v^2 u_{0xx} + v b_1 w_{0x} w_{0xx}) \Big) \delta u_{0x} |_0^L \mathrm{d}t$$
$$+ \int_{t_1}^{t_2} \Big(EI v \Big(b_2 w_{0x}^3$$
$$+ \frac{1}{2} b_1 u_{0x} w_{0x} \Big) \Big) \delta w_{0xx} |_0^L \mathrm{d}t = 0. \tag{43}$$

The constants $b_1, \cdots, b_6$ and $a_i, i = 1, \cdots, 9$ are given by

$$b_1 = \frac{1}{2}(1 - v)(v + 1), \quad b_2 = \frac{v + 1}{4},$$
$$b_3 = \frac{v^4 + 2v + 1}{4v + 2}, \quad b_4 = \frac{v + 1}{4(2v + 1)},$$
$$b_5 = \frac{(v + 1)(v(v^2 + v + 2) + 1)}{4v + 2},$$
$$b_6 = -\frac{3(v + 1)(v(v^3 + v - 1) - 1)}{4v + 2},$$
$$a_1 = -\frac{v^4 + 2v + 1}{2v + 1}, \quad a_2 = v^2 - 1,$$
$$a_3 = \frac{12v^5 + 2v^4 + 7v^3 + 10v^2 - 19v - 12}{8v + 4}$$
$$a_4 = \frac{v^2(v + 1)}{4v + 2}, \quad a_7 = \frac{2v^4 - 2v^3 - 3v^2 + 3v + 2}{4v + 2}$$
$$a_8 = \frac{-6v^5 - 4v^4 - 5v^3 - 2v^2 + 11v + 6}{2v + 1},$$
$$a_6 = -3(v + 1)$$

$$a_9 = \frac{-12v^5 - 10v^4 - 11v^3 - 2v^2 + 23v + 12}{8v + 4}. \tag{44}$$

By the Hamilton principle, Eq. (43) leads to the two following coupled model equations for the problem

$$A \rho u_{0tt} + AE(a_1 u_{0xx} + a_2 w_{0x} w_{0xx} - I \rho v^2 u_{0xxtt})$$
$$+ EI(a_2 w_{0xx} w_{0xxx} + a_3 u_{0xxxx}$$
$$+ a_4 w_{0x} w_{0xxxx}) = 0, \tag{45}$$
$$A P \delta(x - t\gamma) + I P v \delta_{xx}(x - \gamma t) + A \rho w_{0tt}$$
$$+ AE(w_{0x} u_{0xx} + a_1 u_{0x} w_{0xx} + a_5 w_{0x}^2 w_{0xx})$$
$$+ I \rho (v - 1) w_{0xxtt}$$
$$+ EI(a_6 w_{0xx}^2 + a_7 u_{0xx} w_{0xxx} + a_8 u_{0xxx} w_{0xx}$$
$$+ 4 a_6 w_{0x} w_{0xx} w_{0xxx} + a_4 w_{0x} u_{0xxxx}$$
$$+ \frac{1}{2} a_7 u_{0x} w_{0xxxx}$$
$$- a_1 w_{0xxxx} + a_6 w_{0x}^2 w_{0xxxx}) = 0. \tag{46}$$

As can be found from Eq. (43), there are five natural boundary terms

$$\Big(AE(b_1 w_{0x} u_{0x} + 4 b_2 w_{0x}^3)$$
$$+ I \rho \Big(w_{0ttx} - \frac{1}{2} v w_{0xxt} - \frac{1}{2} v w_{0ttx} \Big)$$
$$+ EI(v b_1 w_{0xx} u_{0xx} - v b_1 (w_{0xx} u_{0xx} + w_{0x} u_{0xxx})$$
$$- 2 b_3 w_{0xxx}$$
$$- 2 b_5 w_{0xxx} w_{0x}^2 - 2 b_5 w_{0xx}^2 w_{0x} + 6 v b_2 w_{0x}^2 w_{0xxx}$$
$$+ 6 v b_2 w_{0xx}^2 w_{0x}$$
$$- 2 b_6 (w_{0xxx} u_{0x} + w_{0xx} u_{0xx}) + \frac{1}{2} v b_1 u_{0x} w_{0xxx}$$
$$+ \frac{1}{2} (u_{0xxx} w_{0x}$$
$$+ 2 u_{0xx} w_{0xx} + u_{0x} w_{0xxx}))$$
$$- \frac{1}{2} I P v \delta_x (x - \gamma t)) \delta w_0 |_0^L = 0, \tag{47}$$
$$\Big(AE(b_1 w_{0x}^2 + b_3 u_{0x}) + I \rho v^2 u_{0ttx} - EI(2 b_4 u_{0xxx}$$
$$+ v b_1 (w_{0xx}^2 + w_{0x} w_{0xxx}) - b_6 w_{0xx}^2$$
$$- \frac{1}{2} v b_1 w_{0x} w_{0xxx})) \delta u_0 |_0^L = 0, \tag{48}$$
$$\Big(EI \Big(\frac{1}{2} v b_1 w_{0x} u_{0xx} + 2 b_3 w_{0xx}$$
$$+ (2 b_5 - 3 b_2 v) w_{0x}^2 w_{0xx}$$
$$+ (2 b_6 - v b_1) u_{0x} w_{0xx})) \delta w_{0x} |_0^L = 0. \tag{49}$$
$$\Big(EI(2 b_4 v^2 u_{0xx} + v b_1 w_{0x} w_{0xx})) \delta u_{0x} |_0^L = 0. \tag{50}$$
$$\Big(EI v \Big(b_2 w_{0x}^3 + \frac{1}{2} b_1 u_{0x} w_{0x} \Big) \Big) \delta w_{0xx} |_0^L = 0. \tag{51}$$

The above five natural boundary terms correspond to the five terms u_0, w_0, w_{0x}, u_{0x} and w_{0xx} as involved in (1), which is similar to the case of the vibration problem for Reddy beam in [41]. If the material parameter $v = 0$, the last two boundary conditions (50) and (51) vanish. Further, if the effect of finite deformation is neglected, the remaining boundary conditions (47),(48) and (49) would be exactly the ones for Euler–Bernoulli beam.

In some of the beam theories, the boundary conditions can be expressed in terms of the stress resultants, such as $N = \int_A S_{xx} dA$, $M = \int_A y S_{xy}$ and so on. However, for the model considered in the finite deformation setting in this paper, the stress resultants involved in the boundary conditions such as $\int_A S_{yy} dA$, $\int_A y S_{yy}$, ... are lengthy expressions of the displacements, and the physical meaning is not sound. So, the boundary conditions for the model shall be expressed in terms of the displacements $u(x, t)$ and $w(x, t)$.

The simply supported boundary condition assumes that the two ends of the beam are in-plane immovable. Thus, combining Eqs. (47) and (48), it leads to

$$w_0(x, t) = 0, \quad u_0(x, t) = 0, \quad \text{at} \quad x = 0, L. \quad (52)$$

Furthermore, the bending moment $M(x, t)$ of the beam with simply supported boundaries should be zero at the boundary, which then leads to

$$M(x, t) = \int_A y * S_{xx} dA = 0. \quad \text{at} \quad x = 0, L. \quad (53)$$

After some manipulations, (53) can be rewritten as

$$M(x, t) = \frac{EI(1 + v)^2}{(1 + 2v)} \Big(-vw_{0x}u_{0xx} + \big(\frac{v^2 - 1 - v}{1 + v}$$
$$-\big(1 + \frac{v^3}{1 + v}\big)u_{0x}\big)w_{0xx}\Big) = 0, \quad \text{at} \quad x = 0, L. \quad (54)$$

Equation (54) implies that the cross section of the beam at the boundary can be freely rotated. This yields

$$\frac{\partial u_1(x, y, t)}{\partial y} \neq 0, \quad \text{at} \quad x = 0, L. \quad (55)$$

Based on Eqs. (1), (55) yields the following condition

$$w_{0x}(x, t) \neq 0, \quad \text{at} \quad x = 0, L. \quad (56)$$

With (56), the boundary condition in (49) can be rewritten as

$$\Big(EI\big(\frac{1}{2}vb_1w_{0x}u_{0xx} + 2b_3w_{0xx} + (2b_5 - 3b_2v)w_{0x}^2 w_{0xx}$$
$$+ (2b_6 - vb_1)u_{0x}w_{0xx}\big)\Big) = 0, \quad \text{at} \quad x = 0, L. \quad (57)$$

By eliminating the term $w_{0x}u_{0xx}$ from (54) and (57), it gives

$$\big(a_{13}u_{0x} + a_{14} + a_{15}w_{0x}^2\big)w_{0xx} = 0, \quad \text{at} \quad x = 0, L, \quad (58)$$

where

$$a_{13} = (v - 1)(11 + v(31 + v(28 + v(10v + 19)))),$$
$$a_{14} = -v(6 + v(2 + v(2v + 3))) - 3,$$
$$a_{15} = (-v - 1)(4 + v(4v^2 - 2v + 5)). \quad (59)$$

In view of Eqs. (51) and (58), $w_0(x, t)$ should satisfy the following conditions

$$w_{0xx}(x, t) = 0, \quad \text{at} \quad x = 0, \quad L. \quad (60)$$

From (57), another boundary condition for $u_0(x, t)$ is given by

$$u_{0xx}(x, t) = 0, \quad \text{at} \quad x = 0, \quad L. \quad (61)$$

To summarize, the boundary conditions for a simply supported beam can be given by

$$w_0(x, t) = 0, \quad u_0(x, t) = 0, \quad \text{at} \quad x = 0, \quad L.$$
$$w_{0xx}(x, t) = 0, \quad u_{0xx}(x, t) = 0, \quad \text{at} \quad x = 0, \quad L. \quad (62)$$

References

1. Fryba, L.: Vibration of Solids and Structures under Moving Loads. Noordhoff International Publishing, Groningen (1972)
2. Ouyang, H.: Moving-load dynamic problems: a tutorial (with a brief overview). Mech. Syst. Signal Process. **25**, 2039–2060 (2011)
3. Froio, D., Rizzi, E., Simoes, F.M.F., Costa, A.I.D.: Universal analytical solution of the steady-state response of an infinite beam on a Pasternak elastic foundation under moving load. Int. J. Solids Struct. (2017). https://doi.org/10.1016/j.ijsolstr.2017.10.005
4. Simsek, M.: Vibration analysis of a functionally grade beam under a moving mass by using different beam theories. Compos. Struct. **92**, 904–917 (2010)
5. Ferretti, M., Piccardo, G., Luongo, A.: Weakly nonlinear dynamics of taut strings traveled by single moving force. Meccanica (2017). https://doi.org/10.1007/s11012-017-0690-5
6. Museros, P., Moliner, E., Rodrigo, M.D.M.: Free vibrations of simply-supported beam bridges under moving loads: maximum resonance, cancellation and resonant vertical acceleration. J. Sound Vib. **332**, 326–345 (2013)
7. Nguyen, D.K., Nguyen, Q.H., Tran, T.T., Bui, V.T.: Vibration of bi-dimensional functionally graded Timoshenko beam excited by a moving load. Acta Mech. **228**, 141–155 (2017)

8. Rao, G.V.: Linear dynamics of an elastic beam under moving loads. J. Vib. Acoust. **122**, 281–289 (2000)

9. Kumar, C.P.S., Sujatha, C., Shankar, K.: Vibration of simply supported beams under a single moving load: a detailed study of cancellation phenomenon. Int. J. Mech. Sci. **99**, 40–47 (2015)

10. Kumar, C.P.S., Sujatha, C., Shankar, K.: Vibration of nonuniform beams under moving point loads: an approximate analytical solution in time domain. Int. J. Struct. Stab. **17**, 1750035-1–1750035-17 (2017)

11. Li, S.H., Ren, J.Y.: Analytical study on dynamic responses of a curved beam subjected to three-directional moving loads. Appl. Math. Model. **58**, 365–387 (2018)

12. Sheng, G.G., Wang, X.: The geometrically nonlinear dynamic responses of simply supported beams under moving loads. Appl. Math. Model. **48**, 183–195 (2017)

13. Eftekhari, S.A.: A differential quadrature procedure for linear and nonlinear steady state vibration of infinite beams traversed by a moving point load. Meccanica **51**, 2417–2434 (2016)

14. Lorenzo, S.D., Paola, M.D., Pirrotta, A.: On the moving load problem in Euler–Bernoulli uniform beams with visoelatic supports and joints. Acta Mech. **228**, 805–821 (2017)

15. Timoshenko, S.P.: Method of analysis of statical and dynamical stresses in rail. In: 2nd, International Congress of Applied Mechanics. Zurich, pp. 407–420 (1926)

16. Kenney, J.T.: Steady state vibrations of beam on elastic foundation for moving laod. J. Appl. Mech. **21**, 359–364 (1954)

17. Crandall, S.H.: The Timoshenko beam on an elastic foundation. In: Proceeding of the Third Midwestern Conference on Solid Mechanics, pp. 146–159 (1957)

18. Achenbach, J.D., Sun, C.T.: Moving load on a flexible supported Timoshenko beam. Int. J. Solids Struct. **1**, 353–370 (1965)

19. Steele, C.R.: The Timoshenko beam with a moving load. J. Appl. Mech. **35**, 481–488 (1968)

20. Dieterman, H.A., Metrikine, A.: The equivalent stiffness of a half-space interaction with a beam. Critical velocity of a moving load along the beam. Eur. J. Mech. A Solids **15**, 67–90 (1996)

21. Rodrigues, C., Simões, F.M.F., Pinto da Costa, A., Froio, D., Rizzi, E.: Finite element dynamic analysis of beams on nonlinear elastic foundations under a moving oscillator. Eur. J. Mech. A Solids **68**, 9–24 (2018)

22. Froio, D., Rizzi, E., Simões, F.M.F., Pinto da Costa, A.: Dynamics of a beam on a bilinear elastic foundation under harmonic moving load. Acta Mech. (2018). https://doi.org/10.1007/s00707-018-2213-4

23. Dimitrovovà, Z.: Analysis of the critical velocity of a load moving on a beam supported by a finite depth foundation. Int. J. Solids Struct. (2017). https://doi.org/10.1016/j.ijsolstr.2017.06.009

24. Dimitrovovà, Z., Rodrigues, A.F.S.: Critical velocity of a uniform moving load. Adv. Eng. Softw. **68**, 44–56 (2012)

25. Chang, Yung-Hsiang, Huang, Yen-Hui: Dynamic characteristic of infinite and finite railways to moving loads. J. Eng. Mech. **129**, 987–995 (2003)

26. Tekili, S., Khadri, Y., Merzoug, B.: Free and forced vibration of beams strengthened by composite coats subjected to moving loads. Mech. Compos. Mater. **52**, 789–798 (2017)

27. Kim, T., Park, I., Lee, U.: Forced vibration of a Timoshenko beam subjected to Stationary and moving loads using the modal analysis method. Shock Vib. (2017). https://doi.org/10.1155/2017/3924921

28. Ding, Hu, Shi, Kang-Li, Chen, Li-Qun, Yang, Shao-Pu: Dynamic response of an infinite Timoshenko beam on a nonlinear visoelatic foundation to a moving load. Nonlinear Dyn. **73**, 285–298 (2013)

29. Sapountzakis, E.J., Kampitsis, A.E.: Nonlinear response of shear deformable beams on tensionless nonlinear viscoelastic foundation under moving loads. J. Sound Vib. **330**, 5410–5426 (2011)

30. Tabejieu, L.M.A., Nbendjo, B.R.N., Woato, P.: On the dynamics of Rayleigh beams resting on fractional-order viscoelastic Pasternak foundations subjected to moving loads. Chaos Solitons Fractals **93**, 39–47 (2016)

31. Hryniewicz, Z.: Dynamics of Rayleigh beam on nonlinear foundation due to moving load using Adomian decomposition and coiflet expansion. Soil Dyn. Earthq. Eng. **31**, 1123–1131 (2011)

32. Chen, Yang, Yiming, Fu, Zhong, Jun, Li, Yingli: Nonlinear dynamic responses of functionally graded tubes subjected to moving load based on a refined beam model. Nonlinear Dyn. **88**, 1441–1452 (2017)

33. Zhu, X.W., Wang, Y.B., Lou, Z.M.: A study of the critical strain of hyperelastic materials: a new kinematic frame and the leading order term. Mech. Res. Commun. **78**, 20–24 (2016)

34. Wang, Y.B., Ding, H., Chen, Li-Qun: Nonlinear vibration of axially accelerating hyperelastic beams. Int. J. Non-Linear Mech. **99**, 302–310 (2018)

35. Wickert, J.A.: Nonlinear vibration of a traveling tensioned beam. Int. J. Non-Linear Mech. **27**, 503–517 (1992)

36. Wang, F.F., Dai, Hui-Hui: Asymptotic bifurcation analysis and post-buckling for uniaxial compression of a thin incompressible hyperelastic rectangle. IMA J. Appl. Math. **75**(4), 506–524 (2010)

37. Dai, Hui-Hui, Wang, Y.B., Wang, F.F.: Primary and secondary bifurcations of a compressible hyperelastic layer: asymptotic model equations and solutions. Int. J. Non-Linear Mech. **52**, 58–72 (2013)

38. Wang, F.F., Wang, Y.B.: Buckling and post-buckling of a compressible slab under combined axial compression and lateral load. ZAMM J. Appl. Math. Mech. (2017). https://doi.org/10.1002/zamm.201600115

39. Stephen, N.G., Levinson, M.: A second order beam theory. J. Sound Vib. **67**, 293–305 (1979)

40. Thai, S., Thai, Huu-Tai, et al.: A simple shear deformation theory for nonlocal beams. Compos. Struct. **183**, 262–270 (2018)

41. Reddy, J.N.: Nonlocal theories for bending, buckling and vibration of beam. Int. J. Eng. Sci. **45**, 288–307 (2007)